Towards suppressing H blistering by investigating the physical origin of the H–He interaction in W

IOP Publishing and International Atomic Energy Agency Nuclear Fusion
Nucl. Fusion **50** (2010) 115010 (8pp) doi:10.1088/0029-5515/50/11/115010

Towards suppressing H blistering by investigating the physical origin of the H–He interaction in W

Hong-Bo Zhou[1], Yue-Lin Liu[1], Shuo Jin[1], Ying Zhang[1], G.-N. Luo[2] and Guang-Hong Lu[1]

[1] Department of Physics, Beihang University, Beijing 100191, People's Republic of China
[2] Institute of Plasma Physics, Chinese Academy of Sciences, Hefei 230031, People's Republic of China

E-mail: LGH@buaa.edu.cn (G-H Lu)

Received 5 March 2010, accepted for publication 27 September 2010
Published 25 October 2010
Online at stacks.iop.org/NF/50/115010

Abstract
We investigate the physical origin of H–He interaction in W in terms of optimal charge density by calculating the energetics and diffusion properties using a first-principles method. On the one hand, we show a strong attraction between H and He in W originated from the charge density redistribution due to the presence of He, driving H segregation towards He. This can block the permeation of H into deeper bulk and thus suppress H blistering. On the other hand, we demonstrate that He, rather than H, energetically prefers to occupy the vacancy centre due to its closed-shell structure, which can block H_2 formation at the vacancy centre. This is because He causes a redistribution of charge density inside the vacancy to make it 'not optimal' for the formation of H_2 molecules, which can be treated as a preliminary nucleation of the H bubbles. We thus propose that H retention and blistering in W can be suppressed by doping the noble gas elements.

(Some figures in this article are in colour only in the electronic version)

1. Introduction

Nuclear fusion energy, as an environmentally clean and infinite energy source, is a way to reduce our reliance on fossil fuel sources in the future. Nowadays, energy shortage has driven us to make considerable effort to develop nuclear fusion and thereby it is going to be of practical use in the foreseeable future. Fusion energy is being developed internationally via the International Thermonuclear Experimental Reactor (ITER) Project [1], which aims to demonstrate the extended burn of deuterium–tritium (D–T) plasma in a fusion reaction. The property of plasma-facing materials (PFMs) under D–T plasma irradiation is one of the crucial issues in the use of nuclear fusion energy [2].

W as a high-Z material is considered to be the most promising candidate for PFMs in fusion reactors because of its high melting point, high thermal conductivity and low sputtering yield for light elements [3]. However, as a PFM, W will be exposed to extremely high fluxes of H isotope ions, and He as well as high energy neutrons in a fusion reaction, which lead to blister formation, surface sputtering erosion and displacement damage. Therefore, the mechanical properties and the structural strength of W under H isotope ions and He irradiation are some of the key concerns for W PFM and have been under intensive investigation. So far, solution, accumulation, blister formation and retention behaviours with H or He solely in W have been investigated both experimentally and computationally [4–13]. Detailed descriptions of an individual He or H atom in W have become attainable based on the recent advances in first-principles theory and computing power. An individual H [9] or He [10] atom is calculated to energetically occupy the tetrahedral interstitial site (TIS) in bulk W. Vacancy and grain boundary defects in W serve as trapping centres for H [11, 12] or He [13]. We reveal the microscopic vacancy trapping mechanism for H bubble formation in W with a vacancy defect, which provides an isosurface of optimal charge density that induces collective H binding on its internal surface, a prerequisite for the formation of H_2 molecules and nucleation of H bubbles inside the vacancy [11].

The synergistic effect of H and He is shown to be quite different from that with single H or He irradiation alone [14–18]. The trapping state of H is largely changed by the He ion irradiation in W [14]. After He pre-implantation on W materials, the subsequent H has been observed to accumulate in the He saturated layer [15, 16]. The presence of He increases

D trapping at the near surface, limiting D diffusion into the W bulk [16–18]. D retention can be reduced by as large as ∼50% [14] or ∼70% [17] due to the presence of He depending on the irradiation conditions. However, the presence of D has little effect on He retention [16, 17]. Computationally, only very limited work focused on the synergistic effects of H and He in W [19, 20]. Removing a He atom from H–He–V complexes is found to be more energy consuming than removing a H atom (∼2–3 eV higher), indicating that He substitution in a He–V complex by a H atom is almost impossible [20]. This suggests that He binds more strongly with a vacancy in comparison with H. In a previous work, in Ta, using nuclear reaction analysis and the ion implantation technique, D is found to energetically prefer to occupy the vacancies and internal surfaces of the He bubbles in comparison with the interstitial site [21]. This is because He induces H trapping at the vacancies or the internal surface of He bubbles produced by atomic displacements during the energetic implantation of He. The binding of H is therefore similar to chemisorption of H at clean external surfaces, which one calls a 'chemisorption-like mechanism'. However, the physical intrinsic mechanism for the experimentally observed H trapping by He in W is still unclear.

In this work, we try to explore the physical origin of the H–He interaction in W by investigating the synergistic dissolution and diffusion behaviour of H and He in W using a first-principles method. The revelation of the mechanism is able to pave a theoretical way to suppress H bubble formation in W PFMs.

2. Computational method

Our first-principles calculations were performed using the pseudopotential plane-wave method implemented in the Vienna *Ab-initio* Simulation Package (VASP) code [22, 23] based on density functional theory. We used the generalized gradient approximation of Perdew and Wang [24] and projected augmented wave potentials [25], with a plane wave energy cutoff of 350 eV. A bcc W supercell of 128 atoms containing a monovacancy was used, and their Brillouin zones were sampled with (3 × 3 × 3) ***k***-points by the Monkhorst–Pack scheme [26]. The calculated equilibrium lattice constant is 3.17 Å for bcc W, in good agreement with the corresponding experimental value of 3.16 Å. Both supercell size and atomic positions are relaxed to equilibrium, and energy minimization is continued until the forces on all atoms are converged to less than 10^{-3} eV Å^{-1}.

3. Results and discussion

3.1. Interaction of H and He in intrinsic W

Compared with the octahedral interstitial site (OIS), the TIS has been demonstrated to be the most stable site for H and He in intrinsic W. Table 1 shows that the solution energy of H at the TIS is 0.38 eV lower than that at the OIS [9, 19, 27], in which the zero-point energy (ZPE) of H is not considered. However, the ZPE should be taken into account for the light elements H and He, because it plays an important role in the dissolution behaviour of H and He in bulk W. We examine here the energy state of H in very different environments in bulk W. Our computation shows that the ZPE of H is 0.263 eV and 0.256 eV at the TIS and OIS, respectively. Table 1 suggests that the ZPE of H has a significant effect on the solution energies of H in bulk W, but the relative stability of H at the TIS and the OIS remains unchanged. On the other hand, an individual He atom is also energetically favourable sitting at the TIS in W [10, 19] as shown in table 1, similar to that of H. The ZPE of He is calculated to be 0.078 eV and 0.034 eV at the TIS and the OIS, respectively. Again, the ZPE will not change the order of the relative stability of He at the TIS and the OIS.

Table 1. The calculated ZPE and solution energies (eV) of a H or He atom in W in comparison with the previous studies. All the solution energies are referred to one-half of the energy of a H_2 molecule (−3.38 eV).

Configuration		H_{TIS}	H_{OIS}	He_{TIS}	He_{OIS}
ZPE		0.263	0.256	0.078	0.034
with ZPE	This work	1.00	1.38	6.14	6.37
without ZPE	This work	0.88	1.26	6.07	6.34
	[9]	0.88	1.26	—	—
	[10]	—	—	6.16	6.38
	[19]	0.86	1.26	6.23	6.48

In order to investigate the interaction between H and He in bulk W, one He atom is set at a TIS while the H atom occupies a different TIS. The H solution energy (E_H^{sol}) can be obtained by

$$E_H^{sol} = E_{NW,He(TIS),H(TIS)} - E_{NW,He(TIS)} - \tfrac{1}{2}E_{H_2}, \quad (1)$$

where $E_{NW,He(TIS),H(TIS)}$ is the total energy of bulk W with interstitial He and H atoms, and $E_{NW,He(TIS)}$ is the total energy of bulk W with a single interstitial He atom. The third term $\frac{1}{2}E_{H_2}$ is one-half of the energy of a H_2 molecule (−3.38 eV) according to the present calculation. For the H_2 molecule, the ZPE of H is calculated to be ∼0.135 eV with a vibrational frequency of 4315 cm^{-1}, which agrees reasonably well with the experimental value of 4395 cm^{-1} [28]. In addition, the ZPE of H in the presence of He is ∼0.236–0.263 eV depending on the H–He distance. The ZPE is taken into account for the computation of H solution energy surrounding He.

Figure 1 shows the H solution energy as a function of the H–He distance, which suggests that the existence of He substantially affects the dissolution behaviour of the interstitial H in bulk W. The H–He interaction is repulsive with certain H–He distance that is ∼1.6 Å. Beyond this distance, H gains additional energy due to the presence of He, leading to a lower H solution energy in comparison with that of H at the TIS without He. The solution energy increases with increasing H–He distance, and converges to that of H at the TIS without He at ∼3.4 Å. The lowest solution energy occurs at a H–He distance of 1.95 Å (TIS C, 0.76 eV). Therefore, the binding energy of H–He at the most stable configuration is 0.23 eV, which is consistent with that from Becquart and Domain [20], but 0.09 eV larger than that from Lee *et al* [19]. In addition, the H–He equilibrium distance is intermediate between those of H–H (∼2.2 Å) and He–He (∼1.6 Å) in W [9, 20, 27].

We further investigate the atomic configuration in order to explore the origin of the H solution energy gain due to the presence of He. Our first-principles calculations indicate that the variation in the volume of the supercell induced by the

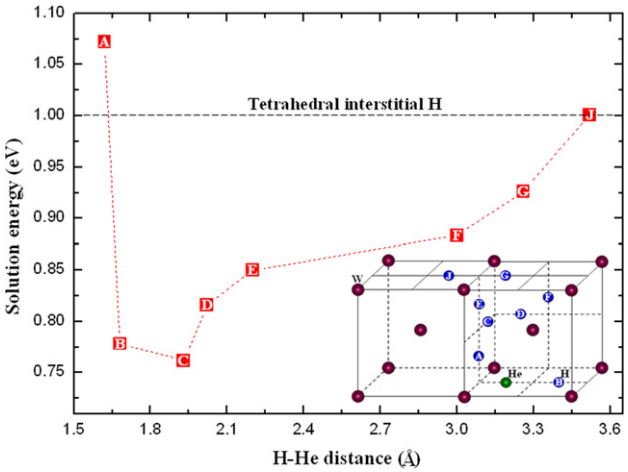

Figure 1. H solution energy in W with He as a function of the H–He distance.

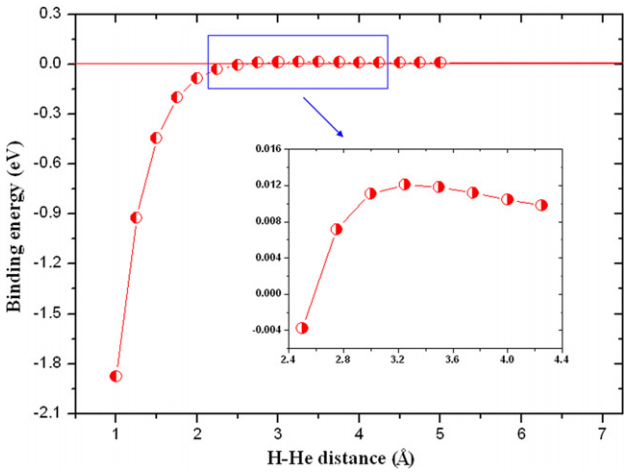

Figure 2. The calculated binding energy (eV) of a H–He pair in vacuum as a function of the H–He spatial separation (Å). Positive values indicate attraction, while negative ones indicate repulsion.

presence of He is so small that it can be neglected. However, the atomic distance between He and the nearest neighbour W extends to 1.94 Å as compared with 1.77 Å for the case without He. Further, the distances between these neighbouring W atoms increase by ∼0.30 Å due to the presence of He at the TIS centre. These suggest the volume expansion of the local TIS with He, which leads to a further expansion of the neighbouring TISs because they share W atom(s) with the TIS with He. For example, as shown in figure 1, the TIS volumes of A–G all extend, but that of J remains unchanged. As a result, the charge density in these TISs decreases due to the volume expansion. Physically, the occupation behaviour of H in a metal can be understood via the optimal charge density [11, 12, 29]. The TIS in W is shown to have an electron density of ∼0.27 electron Å^{-3} [11], which is higher than H prefers to occupy in W. Thus, the lower charge density at the TIS surrounding He due to the volume expansion can reduce the solution energy of H. This is why the TISs of B–G exhibit lower H solution energies due to the presence of He in comparison with that without He (figure 1). For the TIS of C with the lowest solution energy, the charge density is shown to reduce to as low as ∼0.21 electron Å^{-3}. This suggests that He can serve as a trapping centre of H in bulk W by providing a lower charge density for H dissolving, similar to the dissolution behaviour of H in a monovacancy [11]. However, although the TIS of A has a lower charge density (∼0.22 electron Å^{-3}), it exhibits a much higher solution energy. This is because the interaction of H and He for the A case is strongly repulsive due to the shorter H–He interatomic distance (∼1.6 Å). This can be understood by the binding energy as a function of H–He distance in vacuum.

As shown in figure 2, we display the calculated binding energy between free H and He as a function of the H–He interatomic distance in vacuum. It shows a strong repulsive interaction between H and He when their interatomic distance is lower than ∼2.5 Å. Beyond this distance, the binding energy increases rapidly and converges to zero, but experiences a very small peak at a H–He equilibrium distance of ∼3.25 Å with the lowest binding energy of 0.012 eV, 95% lower than the H–He binding energy in W. This implies that a direct interaction between H and He in W can be neglected. Consequently, the strong attraction between H and He in W originates from the charge density redistribution induced by the presence of He. The H–He interaction is quite different from those between two He atoms and two H atoms in W. Previous studies [20, 27] show an elastic interaction between two He atoms with a larger binding energy (∼1.0 eV) and a shorter equilibrium distance (∼1.6 Å). In contrast, the interaction between double H atoms is much weaker with a binding energy of ∼0.01 eV [9, 20, 27].

3.2. Single H at a He–vacancy complex in W

In the previous study, it has been demonstrated that a vacancy can serve as a trapping centre for H due to the strong binding between H and the vacancy [11]. The solution energy of H in a monovacancy is −0.31 eV, which is much lower than that of H at the TIS in bulk W. This is because the vacancy provides an isosurface of low charge density (0.11 electron Å^{-3}), and H energetically prefers to stay on such an isosurface [11]. In addition to H, He is also shown to prefer to occupy the vacancy. The vacancy centre is the most stable site for He in a vacancy with a solution energy of 1.57 eV according to the present calculation. Because H and He coexist in a fusion reactor, we investigate the synergistic behaviour of H and He in W. The H solution energy in the vicinity of a He–vacancy (He–V) complex has been calculated first. The energy minimization finds the most stable site for H to be at an off-He position (∼1.63 Å from He) close to a TIS. H prefers to stay on an isosurface of the same charge density of 0.16 electron Å^{-3} surrounding the He–V complex, as shown in figure 3. The solution energy is the same on the isosurface with 24 minimum sites very close to the TISs. Figure 3(*a*) shows four minimum sites close to the TISs on the front face. The H solution energy at these sites is demonstrated to be −0.07 eV taking into account the ZPE of H at these sites (0.20 eV). This value is 1.07 eV lower than that of H at the TIS in bulk W, while 0.21 eV higher than that at a monovacancy.

According to the above analysis, the optimal charge density of H at the He–V complex is 0.05 electron Å^{-3} higher than that of H in the He-free vacancy. This is because the presence of He changes the charge density distribution at the vacancy. In addition, the configuration effect also

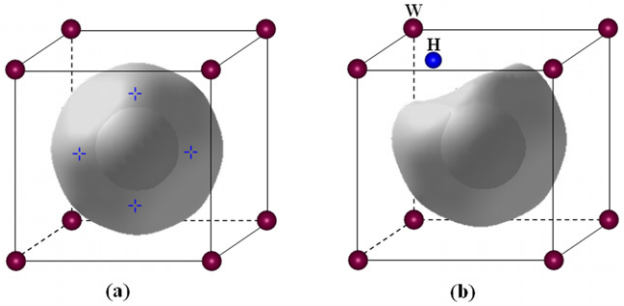

Figure 3. Isosurface of optimal charge density for H binding at a He–V complex: (*a*) without H, (*b*) with one H. The crosses mark the four minimum-energy H binding sites on the front side of the isosurface.

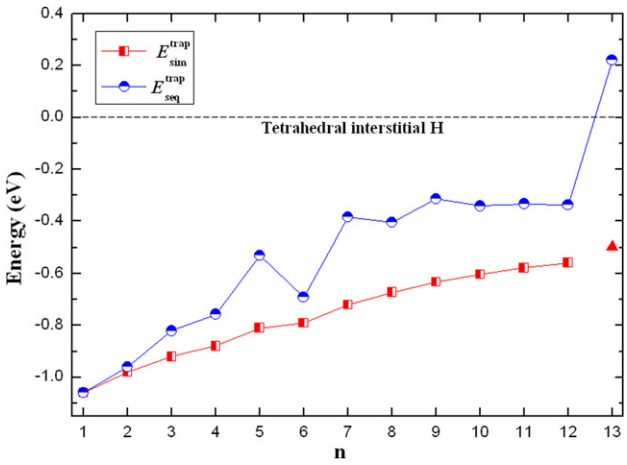

Figure 4. The trapping energy per H as a function of the number of H atoms trapped by the He–V complex in W. The zero point is the energy of H in the TIS far away from the He–V complex.

plays a role because vacancy volume increases by 0.9 Å^3 due to He occupancy at the vacancy centre. Consequently, the isosurface of optimal charge density for H expands from 20.58 to 35.45 Å^2, producing more possible 'optimal charge density sites' for H (24 sites) in comparison with that for a He-free vacancy (6 sites) [11]. Further, the optimal charge density of H provided by the He–V complex is lower than that at the TIS in bulk W by 0.11 electron Å^{-3}, resulting in a stronger binding between the H and He–V complex in comparison with H at the TIS. This implies that the He–V complex can act as a trapping centre which drives segregation of H towards it.

In addition, it can be found in figure 3 that another smaller sphere with a radius of ∼0.8 Å exists, having the same value as the optimal charge density for H (0.16 electron Å^{-3}), which is different from the case for H at the He-free vacancy. Such a sphere appears due to the presence of He. It is not suitable for H to stay owing to a strong repulsive interaction between H and He at this distance as shown in figure 2.

3.3. H trapping surrounding a He–V complex

Theoretically, 24 equivalent most stable sites for H atoms surrounding the He–V complex exist. However, all these sites cannot be occupied together by H because of the H–H repulsive interaction in W [9]. To investigate the trapping of multi-H atoms surrounding the He–V complex in W, we calculate the trapping energy of additional H atoms segregating to the He–V complex and determine the number of H atoms that a He–V complex can accommodate and the stability. We bring the H atoms one by one to the He–V complex and minimize the energy to find the optimal dissolving site at each step. Each H atom occupies, one by one, the 'close-to-TISs' surrounding the He–V complex on the isosurface of optimal charge density. It is important to note that as more H atoms are added, the surface of optimal density shrinks so that there will be less available optimal-density sites to accommodate additional H.

In this work, we try to calculate the number of H atoms that one He–vacancy complex can trap. This depends on the ways of calculating the H trapping energy at the He–vacancy complex. Generally, diffusion of H towards the vacancy in W should be associated with the H concentration. Qualitatively, at a high H concentration, multi-H atoms can diffuse to the He–vacancy complex at the same time (*the simultaneous way*). At a low H concentration, H atoms can diffuse to the He–vacancy complex sequentially (*the sequential way*). As a matter of fact, both ways are used to determine the number of trapping impurity atoms in defects, but there is no direct comparison between these two ways. For example, for H in Al, Lu and Kaxiras [30] demonstrated that a single vacancy can trap 12 H atoms using '*the simultaneous way*', while Ismer *et al* [31] reported that a single vacancy can only trap 8 H atoms using '*the sequential way*'.

For '*the simultaneous way*', the average trapping energy ($E^{\rm trap}_{\rm sim}$) per H atom is defined as

$$E^{\rm trap}_{\rm sim} = \tfrac{1}{n}[E_{(N-1)\rm W,HeV,H_n} - E_{(N-1)\rm W,HeV}] - [E_{N\rm W,H(TIS)} - E_{N\rm W}], \quad (2)$$

where $E_{(N-1)\rm W,HeV,H_n}$ and $E_{(N-1)\rm W,HeV}$ are the total energies of the He–V complex system with and without H atoms, respectively. $E_{N\rm W,H(TIS)}$ and $E_{N\rm W}$ are the energies of the W supercell with and without H atoms, respectively. A negative $E^{\rm trap}_{\rm sim}$ means energy gain when the H atoms are trapped by the He–V complex relative to dispersion into n different TISs. On the other hand, for the '*the sequential way*', the sequential trapping energy ($E^{\rm trap}_{\rm seq}$) per H atom can be obtained by

$$E^{\rm trap}_{\rm seq} = E_{(N-1)\rm W,HeV,H_n} - E_{(N-1)\rm W,HeV,H_{n-1}} - E_{N\rm W,H(TIS)} + E_{N\rm W}. \quad (3)$$

The trapping energy as a function of the number of H trapped by the He–V complex in W is illustrated in figure 4.

For '*the simultaneous way*', according to equation (2), we calculate the average H trapping energy per H atom as a function of the number of H trapped by the He–V complex, as shown in figure 4. The first H atom attains a trapping energy of −1.07 eV as it sits on the optimal charge density isosurface. As more H atoms are added, they experience an interaction of H with each other. The average trapping energy becomes a little lower (−0.97 eV) when the second H atom is embedded in comparison with that of the first one (−1.07 eV). With an increasing number of H atoms, the trapping energy per H atom increases, as shown in figure 4. When the number of H atoms is up to 13, the average H trapping energy is still negative at −0.50 eV. It is lower than that of H at the TIS far away from the He–V complex (set as the ZPE in figure 4), which indicates that the number of H atoms trapped by the He–V

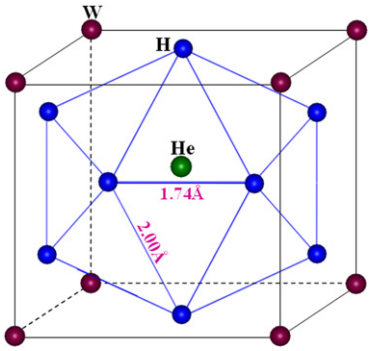

Figure 5. The atomic configuration of the (HeV)H_{12} complex in W.

complex should be larger than 13. After carefully checking the atomic configurations of each H addition, we found that a He–V complex can only accommodate 12 H atoms. The 13th embedded H atom will fall into one of the TISs out of the vacancy, although the average H trapping energy is still lower than that of H in the TIS.

On the other hand, '*the sequential way*' gives different results. As illustrated in figure 4, with an increasing number of H atoms added from 1 to 5, the trapping energy increases. It is important to note that the trapping energy becomes lower (−0.69 eV) when the 6th H atom is added in comparison with the 5th one (−0.53 eV), suggesting that (HeV)H_6 is stabler than (HeV)H_5 in W. This may be attributed to the fact that the symmetry of (HeV)H_6 is higher than that of (HeV)H_5. When the 7th H atom is added, the trapping energy is much larger than that of the 6th H atom by 0.31 eV. After the 7th H atom is added, the variation of trapping energies becomes weak until the 13th H atom is added, and even slowly decreases from 9th to 12th. Similar results were also given by a recent first-principles study [32]. Finally, the 13th H atom addition gives rise to a positive trapping energy of 0.22 eV in reference to that of H at the TIS in bulk W. This suggests that the 13th H atom will prefer to occupy the TIS in bulk W rather than the He–V complex. Therefore, the maximal number of H atoms that can be trapped by the He–V complex is 12 via '*the sequential way*'.

We show the above two different ways to bring the H atoms into a He–V complex, showing different trapping energetics. However, one He–V complex can hold up to 12 H atoms, independent of the trapping ways. Atomic configurations show that the shortest distance between H atoms is always much longer than that of the H_2 molecule (0.75 Å). This implies no H_2 molecule forms with He at the vacancy centre. Interestingly, H forms an icosahedron in the (HeV)H_{12} complex, as shown in figure 5. The icosahedron consists of 12 isosceles and 8 equilateral triangles. The distance between H and its 1NN is ∼1.74 Å, and that between H and its 2NN is ∼2.00 Å. As a comparison, the equilibrium H–H distance in W is ∼2.2 Å [9, 20, 27].

3.4. H diffusion into a He–V complex

Clearly, the above results demonstrate the thermodynamic feasibility of H segregation towards the He–V complex trap so as to initiate a stable complex (HeV)H_{12}. Next, we will investigate the kinetic process for such a trapping. We calculated the energy barriers for H atoms diffusing one by one from a far-away bulk TIS to the He–V complex. We used a drag method relaxing the atomic positions constrained in a hyperplane perpendicular to the vector from the initial to the final position [33].

In our previous investigation, it was found that the optimal diffusion path of H is TIS → TIS with a diffusion energy barrier of 0.20 eV in the intrinsic bulk W [9]. Away from the He–V complex, H atoms also jump from one TIS to another with the same diffusion energy for H in the intrinsic bulk W. As they move close towards the He–V complex, the diffusion barrier is reduced to 0.18 eV from the 3NN (site 1) to 2NN (site 2) TIS and 0.15 eV from the 2NN to 1NN (site 3) TIS of the He–V complex, respectively, as shown in figure 6(*a*). H jumps into the He–V complex from the 1NN TIS into the He–V complex occupying site 4 (figure 6(*a*)), one of the 24 minimum sites at the isosurface of optimal charge density (figure 3), with a much reduced barrier of 0.06 eV. Obviously, the barrier as well as the site solution energy of H become lower with H approaching the He–V complex. The first 6 H atoms will diffuse into the He–V complex via the same diffusion barrier as the first H from the six different faces (up and down, back and front, left and right). It is important to note that the 1NN TIS of the He–V complex is no longer a local stable site for H shown in figure 6, different from the TIS in bulk W.

On the other hand, the 7th–12th H atoms will diffuse into the He–V complex via a similar way but differently from the first six atoms, since the 6 H atoms exist close to six different faces. We take the 12th H atom as an example. As shown in figure 6(*b*), when it moves close towards the (HeV)H_{11} complex, the diffusion barrier is also 0.18 eV from the 3NN (site 1′) to 2NN (site 2′) TIS of the He–V complex, similar to the first H atom. However, other diffusion barriers become 0.19 eV and 0.12 eV, respectively. They are higher than that of the first H by 0.04 eV and 0.06 eV, respectively, but still lower than that in bulk W. This suggests that H diffusion into the He–V complex is kinetically feasible.

3.5. Competency of H and He occupation at a vacancy in W

As mentioned in section 1, H and He coexist in nuclear fusion reactions. Now we investigate the capability of H and He to occupy a vacancy in W, which plays an important role in the understanding of the interaction between H and He. Energetically, a vacancy can provide stable sites for H in W [11]. The most stable site for H in a vacancy is found to be at an off-vacancy-centre position (∼1.28 Å from the vacancy centre) close to an OIS with a solution energy of −0.31 eV. As mentioned above, the vacancy centre is the most stable site for He in a vacancy with a solution energy of 1.57 eV according to the present calculation. However, the binding energies for H and He with the vacancy are 1.18 eV and 4.59 eV with respect to their solution energies at the TIS in W, respectively. This suggests that He can segregate towards the vacancy from the interstitial site much more easily than H. Therefore, He is more energetically favourable to occupy the vacancy in comparison with H.

The above results demonstrate the thermodynamic feasibility of He segregation towards a vacancy trap. Kinetically, one should explore the process in order to understand how He diffuses into the vacancy. Although He

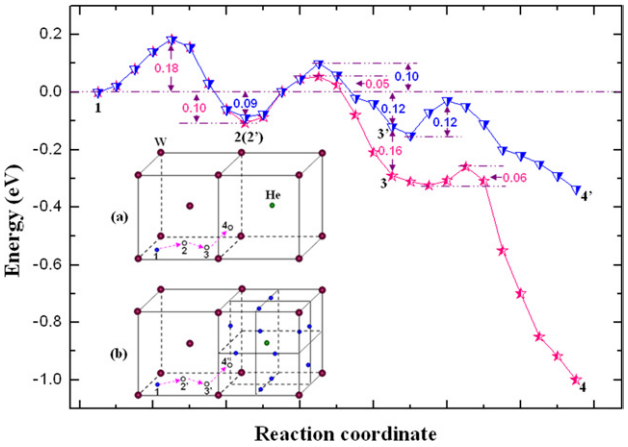

Figure 6. H diffusion energy profile and diffusion paths (arrows) in W with the He–V complex. (*a*) H diffusion towards the most stable site surrounding the He–V complex. Sites 1, 2 and 3 are the 3NN, 2NN and 1NN TIS of the He–V complex, respectively. Site 4 represents the most stable site of H surrounding the He–V complex. (*b*) H diffusion towards the He–V complex with 11 H. Sites 1, 2' and 3' are the 3NN, 2NN and 1NN of the (HeV)H_{11} complex, respectively. Site 4' is the most stable site for the 12th H.

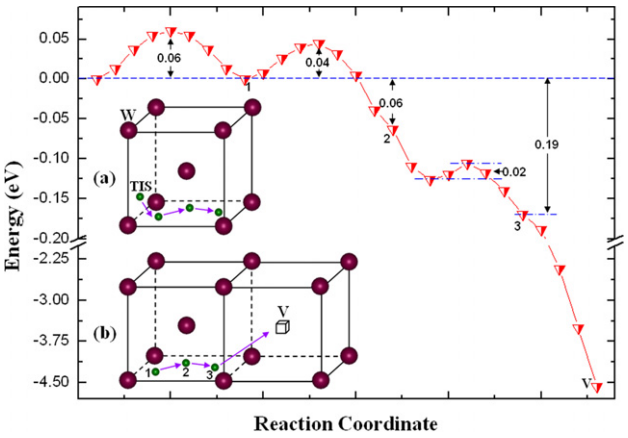

Figure 7. He diffusion energy profile and diffusion paths (arrows) in W. (*a*) He diffusion from one TIS to another in the intrinsic bulk W. (*b*) H diffusion towards an empty vacancy. Sites 1, 2 and 3 are the 3NN, 2NN and 1NN TIS of the vacancy, respectively.

is difficult to diffuse out of the vacancy due to a large binding energy, the kinetic process for He jumping in is actually quite important. Therefore, we calculate the energy barriers for He atoms diffusing from a bulk TIS to the vacancy.

As shown in figure 7(*a*), the optimal diffusion path is the TIS → TIS path with a diffusion barrier of 0.06 eV for He away from the vacancy. This is consistent with He diffusion behaviour in bulk W [10]. As illustrated in figure 7(*b*), when He moves closer to a vacancy, the He diffusion barriers are reduced to 0.04 eV and 0.02 eV, respectively, via the path from the 3NN (site 1), 2NN TIS (site 2) to 1NN (site 3) TIS of the vacancy. There is no diffusion barrier as He jumps into the vacancy from the 1NN TIS, which indicates a downhill 'drift' diffusion of He towards the vacancy. Therefore, the diffusion barrier for He atoms diffusing one by one from a far-away bulk TIS to the vacancy is 0.06 eV, which is much lower than that of H by 0.14 eV. This suggests that He can very easily diffuse into the vacancy. In addition, figure 7 also indicates that the

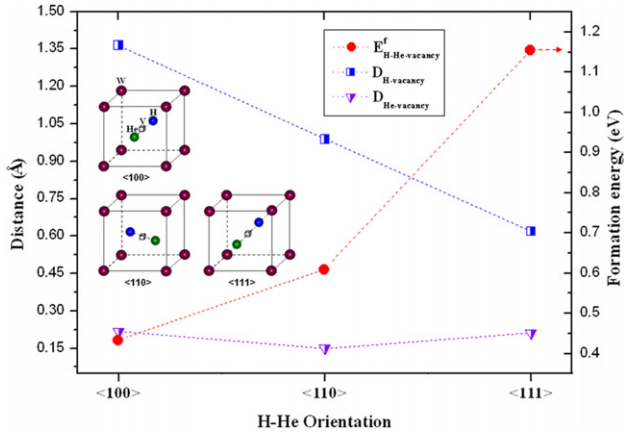

Figure 8. The distance of the H–vacancy centre and the He–vacancy centre, and the formation energy for H and He arrayed along the ⟨1 0 0⟩, ⟨1 1 0⟩ and ⟨1 1 1⟩ directions at the vacancy in W, respectively. The lines are guides to the eye.

1NN and 2NN TIS of the vacancy is no longer the local stable site for He due to the presence of vacancy.

It is clear that single He diffuses very fast in W (0.06 eV). However, He can easily bind with other defects with larger binding energies. For example, He can bind with itself (di-He cluster) with a binding energy of ∼1.0 eV [10]. According to the present calculation, He can bind with H and a vacancy with binding energies of 0.23 eV and 4.59 eV, respectively. Such a binding with defects will surely increase the diffusion barrier of He. Actually, the experimental results gave the diffusion barrier of He as 0.24–0.38 eV [34, 35], which is comparable to that of H in W. Hence, He can be stabilized by binding itself with other defects (particularly a vacancy) in W to form a He-defect cluster. This can also be one of the reasons for the formation of He blisters close to the surface [6, 7]. With this stabilization, the He-defect clusters such as He–He, He–H and He–vacancy can trap H atoms, as illustrated above.

Further, one H atom and one He atom with different configurations in the ⟨1 0 0⟩, ⟨1 1 0⟩ and ⟨1 1 1⟩ directions at the vacancy are investigated to compare the capability of occupying the vacancy of H with that of He. The formation energy of the H–V–He system is calculated by

$$E^{\mathrm{f}} = E_{(N-1)\mathrm{W,HeVH}} - E_{(N-1)\mathrm{W,V}} - E_{\mathrm{He}} - \tfrac{1}{2}E_{\mathrm{H_2}}, \qquad (4)$$

where $E_{(N-1)\mathrm{W,HeVH}}$ and $E_{(N-1)\mathrm{W,V}}$ are the total energy of the supercell with and without H and He atoms, respectively. Figure 8 indicates that H and He atoms at the vacancy in the ⟨1 0 0⟩ dumbbell are most stable for the H–V–He complex, the formation energy of which is lower than that of the H–He ⟨1 1 0⟩ and ⟨1 1 1⟩ dumbbells by 0.18 eV and 0.72 eV, respectively. In the initial H–He dumbbell structure along each direction, the distance between H and the vacancy centre is the same as that of He and the vacancy centre. However, after structure optimization, the H–vacancy centre distance becomes much longer than that of the He–vacancy centre in all cases, as shown in figure 8. He stays close to the vacancy centre, while H deviates from the centre. The largest difference occurs in the H–V–He most stable structure (⟨1 0 0⟩ dumbbell). In this case, the distance between H and the vacancy centre is up to 1.15 Å, while that between He and the vacancy centre is only

0.21 Å. These results suggest that He prefers to occupy the vacancy centre for the H and He coexistence case. In addition, He does not stay right at the centre of the vacancy due to the presence of H. H makes a charge variation inside the vacancy, causing the lowest charge point to deviate from the vacancy centre.

In summary, our density functional theory calculations demonstrate that, as compared with H, (i) He is more energetically favourable to occupy the vacancy; (ii) He exhibits a lower diffusion barrier; and (iii) He is more likely to stay at the vacancy centre. These are consistent with the experimental observations that He prefers to occupy the vacancy and blister rather than H under simultaneous irradiation of H and He [16, 18].

3.6. How to suppress H blistering?

As discussed above, He can be stabilized by binding itself with other defects in W to form He-defect clusters. On the one hand, the vacancy centre is the most stable site for He with a solution energy of 1.57 eV according to the present calculation (section 3.2), since He prefers to occupy the sites with the lowest charge density that is optimal for it. Moreover, He is more competitive to occupy the vacancy in comparison with H (section 3.5). On the other hand, with this stabilization, the He-defect clusters such as He–He and He–vacancy can trap H. Similarly, He bubble should also be able to trap H at its internal surface, as suggested in the previous study [21].

According to the previous first-principles study [11], a vacancy can serve as a trapping centre for H due to a strong binding between H and the vacancy, because the vacancy provides an optimal charge density (0.11 electron $Å^{-3}$) for H. It is energetically favourable for a monovacancy to trap as many as 10 H until a H_2 molecule is formed at the centre of the vacancy. The present calculation shows that no H_2 molecule forms inside a He–V complex (section 3.3), although the number of H atoms trapped by the complex is more than that by a He-free vacancy, quite different from H at the He-free vacancy [11]. This suggests that He can block the formation of H_2 molecules because the prerequisite space and thus the optimal charge density for the formation of H_2 molecules no longer exist due to the presence of He.

Experimentally, D blistering is suppressed in W exposed to a mixed plasma of D and He according to the scanning electron microscopy observations using the linear plasma generator PISCES-A [36]. D retention is shown to be reduced with the formation of nano-sized high-density He bubbles in the near surface [36]. Moreover, both simultaneous and sequential implantation of He and D ions result in D accumulation surrounding the defects containing He near the surface, and the formation of D bubbles is significantly suppressed [16–18]. D retention can be reduced by as large as ∼50% [14] or ∼70% [17] due to the presence of He depending on the irradiation conditions. Further, the He concentration in the D–He mixed plasma/ions lower than 5% can significantly suppress D blistering in W [18, 36].

We believe that the experimentally observed H blistering suppression by He originates from two aspects. On the one hand, He prefers to bind with defects such as a vacancy to block the formation of H_2 molecules, and thus effectively suppress the H bubble formation. On the other hand, a strong attraction between H and a He-defect cluster in W drives H segregation towards He, leading to the accumulation of H surrounding He in the near-surface region. This can block the permeation of H into deeper bulk and thus suppress the H bubble formation. Despite two different mechanisms, both contribute to suppress H blistering in W.

Regarding the blistering depth, Alimov *et al* reported that, without He, the depth for trapped deuterium (D) can be divided into three zones, i.e. (i) the near-surface layer (up to a depth of ∼0.2 μm), (ii) the sub-surface layer (from ∼0.5 to ∼2 μm) and (iii) the bulk (>5 μm) [37]. Other experimental studies on D trapping also show D blistering at the near surface [37–40]. For He, it forms bubbles at the near surface in the range 0–2 μm [6, 41, 42], overlapping with that of the H bubbles' region. Consequently, He can suppress H blistering of W in the near-surface region, as observed experimentally [16–18, 36]. However, a large number of H isotopes will go into W first at the beginning of the fusion reaction, leading to the H (D/T) bubble formation through the near surface to the inner region of W. In this case, H blistering suppression can be realized by pre-implanting the He ions into the inner part of W via adjusting the ion energy so that He can reach the depth one predicts.

It should be noted that a low concentration of He (or He bubble) at the near surface will not effectively block the permeation of H into deeper bulk, because H will continue to diffuse in after the trapping saturation of H by He. This can be solved by using ion-implanting to specially make a He buffer layer, the He density of which is sufficiently high to be capable of trapping H effectively and thus blocks the H permeation.

The proposed 'H-blistering suppressing mechanism' above can also be generalized to other vacancy-related defects such as grain boundaries (GBs) as long as these defects can provide enough space and thus an optimal charge density to hold H, as illustrated in our previous work [11]. Consequently, H GB blistering will be suppressed in the presence of He at the GB. It is shown experimentally that the H bubbles form at the GB of W [43, 44], and H can permeate across the GB into the deeper sites. This is because the diffusion barrier at the GB will be lower in comparison with that in the bulk. As shown in our previous calculations [12], the presence of GB makes the diffusion energy barriers of H reduce to 0.13–0.16 eV from the original 0.20 eV in the bulk. In addition, as a matter of fact, we found that the intrinsic GB cannot provide enough space for holding enough H to form H_2 molecules, suggesting that the vacancy plays a key role in H blistering in a GB [12].

In addition, it is suggested that the nano-sized He bubbles in the near surface of W act as a buffer layer to block D diffusion into the deeper bulk [36]. This should be due to D accumulation surrounding these He bubbles [16–18] as long as the He bubble is sufficiently small. However, if the He bubble is large enough and the He concentration in the He bubble is low, another mechanism that a H_2 molecule forms inside the He bubble at the near surface and then is released may work as well.

Finally, we point out that He blistering in W is also quite harmful, similar to H blistering. This can be solved by replacing He by other inert gas elements. Noble gas elements including neon (Ne) and argon (Ar) can have effects similar to those of He, which can be predicted to effectively suppress H blistering.

4. Conclusions

We have investigated the synergistic behaviour of H and He in W by calculating their energetics and diffusion properties using a first-principles method. We show a strong attraction between H and He in W originated from the charge density redistribution due to the presence of He, driving H segregation towards He, consistent with experimental observations. The binding energy of H with He in the TIS in W is +0.23 eV, and that of H with the He–V complex is +1.00 eV. We demonstrate that a He–V complex can provide a larger isosurface with an optimal charge density of 0.16 electron $Å^{-3}$ in comparison with H in the He-free vacancy. The maximal number of H atoms that can be trapped by such a He–V complex is 12, and H diffusion into the He–V complex is kinetically feasible.

We show that the binding of He and the vacancy is much stronger with a binding energy of +4.59 eV than that of H and the vacancy (+1.18 eV). He exhibits a lower diffusion barrier and is more likely to occupy the vacancy centre due to its closed-shell structure as compared with H. We demonstrate that He can suppress H blistering in two ways. On the one hand, He is able to block the formation of H_2 at the vacancy centre because He causes a redistribution of charge density inside the vacancy to make it 'not optimal' for the formation of H_2 molecules. On the other hand, accumulation of H surrounding He due to the H–He strong attraction in W blocks the permeation of H into deeper bulk and thus suppresses H blistering. We thus suggest that H retention and blistering in W can be suppressed by doping noble gas elements with a closed-shell structure such as Ne and Ar.

Acknowledgments

This research is supported by the National Magnetic Confinement Fusion Program through Grant No 2009GB106003 and the National Natural Science Foundation of China (NSFC) through Grant No 50871009. Hong-Bo Zhou acknowledges the support of the Innovation Foundation of BUAA for PhD Graduates. The authors also acknowledge the helpful discussion with Professor Feng Liu at the University of Utah.

References

[1] Causey R., Wilson K., Venhaus T. and Wampler W.R. 1999 *J. Nucl. Mater.* **266–269** 467
[2] Roth J. *et al* 2009 *J. Nucl. Mater.* **390–391** 1
[3] Janeschitz G. 2001 *J. Nucl. Mater.* **290–293** 1
[4] O'hira S., Steinér A., Nakamura H., Causey R., Nishi M. and Willms S. 1998 *J. Nucl. Mater.* **258–263** 990
[5] Ueda Y., Funabiki T., Shimada T., Fukumoto K., Kurishita H. and Nishikawa M. 2005 *J. Nucl. Mater.* **337–339** 1010
[6] Gilliam S.B., Gidcumb S.M., Parikh N.R., Forsythe D.G., Patnaik B.K., Hunn J.D., Snead L.L. and Lamaze G.P. 2005 *J. Nucl. Mater.* **347** 289
[7] Gilliam S.B., Gidcumb S.M., Forsythe D., Parikh N.R., Hunn J.D., Snead L.L. and Lamaze G.P. 2005 *Nucl. Instrum. Methods Phys. Res.* B **241** 491
[8] Xu Q., Yoshida N. and Yoshiie T. 2007 *J. Nucl. Mater.* **367–370** 806
[9] Liu Y.L., Zhang Y., Luo G.N. and Lu G.H. 2009 *J. Nucl. Mater.* **390–391** 1032
[10] Becquart C.S. and Domain C. 2006 *Phys. Rev. Lett.* **97** 196402
[11] Liu Y.L., Zhang Y., Zhou H.B., Lu G.H., Liu F. and Luo G.N. 2009 *Phys. Rev.* B **79** 172103
[12] Zhou H.B., Liu Y.L., Zhang Y., Jin S., Luo G.N. and Lu G.H. 2010 *Nucl. Fusion* **50** 025016
[13] Zhou H.B., Liu Y.L., Zhang Y., Jin S. and Lu G.H. 2009 *Nucl. Instrum. Methods Phys. Res.* B **267** 3189
[14] Hino T., Koyama K., Yamauchi Y. and Hirohata Y. 1998 *Fusion Eng. Des.* **39–40** 227
[15] Iwakiri H., Morishita K. and Yoshida N. 2002 *J. Nucl. Mater.* **307–311** 135
[16] Lee H.T., Haasz A.A., Davis J.W., Macaulay-Newcombe R.G., Whyte D.G. and Wright G.M. 2007 *J. Nucl. Mater.* **363–365** 898
[17] Lee H.T., Haasz A.A., Davis J.W. and Macaulay-Newcombe R.G. 2007 *J. Nucl. Mater.* **360** 196
[18] Ueda Y., Fukumoto M., Yoshida J., Ohtsuka Y., Akiyoshi R., Iwakiri H. and Yoshida N. 2009 *J. Nucl. Mater.* **386–388** 725
[19] Lee S.C., Choi J.H. and Lee J.G. 2009 *J. Nucl. Mater.* **383** 244
[20] Becquart C.S. and Domain C. 2009 *J. Nucl. Mater.* **386–388** 109
[21] Lee S.R., Myers S.M. and Spulak R.G. 1989 *J. Appl. Phys.* **66** 1137
[22] Kresse G. and Hafner J. 1993 *Phys. Rev.* B **47** 558
[23] Kresse G. and Furthmüller J. 1996 *Phys. Rev.* B **54** 11169
[24] Perdew J.P. and Wang Y. 1992 *Phys. Rev.* B **45** 13244
[25] Blochl P.E. 1994 *Phys. Rev.* B **50** 17953
[26] Monkhorst H.J. and Pack J.D. 1976 *Phys. Rev.* B **13** 5188
[27] Henriksson K.O.E., Nordlund K., Krasheninnikov A. and Keinonen J. 2005 *Appl. Phys. Lett.* **87** 163113
[28] Huber K.P. and Hertzberg G. 1979 *Molecular Spectra and Molecular Structure IV: Constants of Diatomic Molecules* (New York: Van Norstrand Reinhold)
[29] Puska M.J., Nieminen R.M. and Manninen M. 1981 *Phys. Rev.* B **24** 3037
[30] Lu G. and Kaxiras E. 2005 *Phys. Rev. Lett.* **94** 155501
[31] Ismer L., Park M.S., Janotti A. and Van de Walle C.G. 2009 *Phys. Rev.* B **80** 184110
[32] Jiang B., Wan F.R. and Geng W.T. 2010 *Phys. Rev.* B **81** 134112
[33] Fu C.C., Willaime F. and Ordejon P. 2004 *Phys. Rev. Lett.* **92** 175503
[34] Wagner A. and Seidman D.N. 1979 *Phys. Rev. Lett.* **42** 515
[35] Amano J. and Seidman D. 1984 *J. Appl. Phys.* **56** 983
[36] Miyamoto M., Nishijima D., Ueda Y., Doerner R.P., Kurishita H., Baldwin M.J., Morito S., Ono K. and Hanna J. 2009 *Nucl. Fusion* **49** 065035
[37] Alimov V.K., Roth J. and Mayer M. 2005 *J. Nucl. Mater.* **337–339** 619
[38] Tokunaga K., Takayama M., Muroga T. and Yoshida N. 1995 *J. Nucl. Mater.* **220–222** 800
[39] Poon M., Macaulay-Newcombe R.G., Davis J.W. and Haasz A.A. 2005 *J. Nucl. Mater.* **337–339** 629
[40] Tokunaga K., Baldwin M.J., Doerner R.P., Noda N., Kubota Y., Yoshida N., Sogabe T., Kato T. and Schedler B. 2005 *J. Nucl. Mater.* **337–339** 887
[41] Nishijima D., Ye M.Y., Ohno N. and Takamura S. 2003 *J. Nucl. Mater.* **313–316** 97
[42] Debelle A., Barthe M.F., Sauvage T., Belamhawal R., Chelgoum A., Desgardin P. and Labrim H. 2007 *J. Nucl. Mater.* **362** 181
[43] Haasz A.A., Poon M. and Davis J.W. 1999 *J. Nucl. Mater.* **266–269** 520
[44] Causey R.A. 2002 *J. Nucl. Mater.* **300** 91